Title

DETECTION OF NITROGEN ATOMS IN THE 2s(2p)33s 6S5/2 METASTABLE AUTO-IONIZING STATE

Authors

Fairchild, Clifford E.
Garg, Hari P.
Johnson, Charles E.

Publication Date

1973-03-01

Submitted to The Physical Review

LBL-1735
Preprint c.1

DETECTION OF NITROGEN ATOMS IN THE $2s(2p)^3 3s\ ^6S_{5/2}$ METASTABLE AUTO-IONIZING STATE

Clifford E. Fairchild, Hari P. Garg,
and Charles E. Johnson

March 1973

Prepared for the U. S. Atomic Energy
Commission under Contract W-7405-ENG-48

DISCLAIMER

LBL-1735

Submitted to The Physical Review

Detection of Nitrogen Atoms in the $2s(2p)^3 3s\ ^6S_{5/2}$ Metastable Auto-ionizing State

Clifford E. Fairchild* and Hari P. Garg*
Department of Physics
Oregon State University, Corvallis, Oregon 97331

and

Charles E. Johnson†
Lawrence Berkeley Laboratory
University of California, Berkeley, California 94720

March 1973

ABSTRACT

Metastable nitrogen atoms, produced by electron impact dissociation of N_2, have been detected in time-of-flight apparatuses located at OSU and at UC Berkeley. Two different types of metastable atoms are detected; one type resembles Rydberg hydrogen atoms, while the other does not. The measured natural lifetime for the non-Rydberg atoms is 100 ± 25 μsec. Additional information regarding the identity of both types of metastable atoms is obtained by observing their quenching in a static electric field. The field dependent decay constant for the Rydberg atoms is essentially a step function, and these atoms are entirely quenched by a field of 1.5 kV/cm. Both results are consistent with theory if the Rydberg atoms are in levels with principal

quantum number greater than 25. The field dependent decay constant for the non-Rydberg atoms varies quadratically with the strength of the applied electric field. In a field of 4 kV/cm applied along a 6 cm length of flight path, the value of this decay constant is $0.3 \times 10^{6} sec^{-1}$. The quenching results, together with the lifetime measurement, are a strong indication that the non-Rydberg atoms detected in the time-of-flight spectra are nitrogen atoms in the $2s(2p)^{3}3s\ ^{6}S_{5/2}$ metastable auto-ionizing state.

I. INTRODUCTION

Although several measurements involving direct observation of neutral fragments produced by dissociation of simple molecules have been reported in detail[1-9] during the past six years, studies of the dissociation of N_2 have been reported only briefly[10,11]. In both experiments on N_2, the nitrogen molecules were dissociated by electron impact, with electron energies variable from threshold to 200 eV. The energy threshold for the detection of neutral atoms in each experiment was approximately 25 eV, indicating dissociation into a ground state atom and a metastable partner with several eV of internal excitation energy. The highly excited partner was identified as a nitrogen atom in a Rydberg state.

The purpose of the present paper is to describe new measurements of the dissociative excitation of N_2 by electron impact. These new results indicate strongly that a significant fraction of the excited neutral dissociation fragments are atoms in non-Rydberg states. It will also be shown that the detected fragments are not nitrogen atoms in the low lying ^2D and ^2P metastable states; therefore, it is concluded that nitrogen atoms in the $2s(2p)^3 3s\ ^6S_{5/2}$ metastable auto-ionizing state are being detected in addition to atoms in Rydberg states.

II. METHOD

The products of a molecular dissociation process share a kinetic energy which is substantially larger than the ambient mean thermal kinetic energy; therefore it is often possible to isolate, and to some extent, identify dissociation fragments using the time-of-flight technique.[1-9] The simplest configuration of the time-of-flight apparatus used in the present experiment is shown in Fig. 1. The slits serve to define a flight path between the electron bombardment region and the detector (labelled CEM in Fig. 1), and allow differential pumping between the two regions. The gas pressure at the detector is usually at least a factor of ten lower than it is at the electron gun. Also the gas pressure is sufficiently low so that the gas kinetic mean free path, for neutral ground state particles, is greater than the distance from the electron gun to the detector.

For the apparatus shown in Fig. 1, a time-of-flight measurement is made by bombarding N_2 gas in the electron gun region with a short burst of electrons, and simultaneously starting the charging ramp of a time-to-amplitude converter (TAC). The TAC ramp is stopped by a pulse from the detector. If this STOP pulse is initiated by a particle originally produced or excited by the electron gun pulse, then the particle's time-of-flight is proportional to the amplitude of the corresonding output pulse from the TAC. Output pulses from the TAC are stored in a pulse-height analyzer, and a time-of-flight spectrum is accumulated by regular repetition of the electron gun pulse. It is noteworthy that, in order for this spectrum to represent the velocity distribution of particles produced at the electron gun, the total count rate must be so low that the probability for the

occurrence of two or more detector pulses during one cycle of operation is negligible. The electron gun repetition rate is typically 2000 sec^{-1}, and the total count rate is always less than 200 sec^{-1}. In the present experiment, slow metastable N_2 molecules require approximately 0.5 msec to reach the detector and therefore determine the maximum repetion rate.

A windowless electron multiplier used as a detector is sensitive to photons, neutral metastable atoms or molecules, and either positively or negatively charged particles. Using this type of detector biased against negatively charged particles, a typical time-of-flight (TOF) spectrum will include the following different kinds of particles arriving at the detector in order of increasing time-of-flight:

(1) photons emitted from the excitation region during the electron gun pulse;

(2) positive ions, accelerated in the electron gun to several electron volts of kinetic energy during the electron gun pulse, and accelerated again, at the end of the flight path, into the multiplier cathode;

(3) metastable dissociation fragments;

(4) metastable molecules of the parent gas.

Although there are often other events which appear in the TOF spectrum, the above example serves to illustrate that analysis by time-of-flight may be used for particle identification. Additional information is obtained by varying the voltage of the electron gun pulse to examine the threshold for the various spectra. For example, with N_2 as the parent gas, the spectra described above would appear with increasing electron gun pulse height in the order (1), (4), (2) and (3).

III. APPARATUS

A. Vacuum System

The electron gun and about three fourths of the flight path are enclosed in a 2-liter cylindrical stainless steel chamber, which is pumped through a Sorbent A filled pellet trap by a 2-inch stainless steel oil diffusion pump (see Fig. 1). The remaining fourth of the flight path and the detector are enclosed in a 1-liter cylindrical stainless steel chamber welded to the 2-liter chamber and pumped by an 8 ℓ/sec Vac-Ion pump. The foreline is trapped with a liquid nitrogen trap. The base pressure of this system, which has not been baked, is about 2×10^{-7} Torr.

A large pressure differential is maintained between the electron gun region and the detector during an experiment. For the apparatus configuration shown in Fig. 1, the differential pumping is achieved by totally enclosing the flight path between two collimating slits located at both ends of a 0.5 inch diameter stainless steel tube. This tube is pumped out by the Vac-Ion pump at one end, and by the diffusion pump at the other end. Thus, the N_2 target gas entering the electron gun also fills the 2-liter chamber. For the configuration shown in Fig. 2, the flight path is not enclosed; instead the 2-liter chamber is divided by a partition which separates the electron gun from the flight path. Also, the target gas enters the electron gun perpendicular to the flight path.

For both configurations, the pressure of N_2 target gas at the electron gun can be varied from 5×10^{-6} to 2×10^{-4} Torr, while the pressure at the detector is usually at least a factor of ten lower than at the electron gun. Research grade nitrogen is used, and the gas handling system, including the pressure reduction valve, is

stainless steel, except for the gaskets.

B. Electron Gun

The electron gun consists of the cathode, control grid, and screen grid removed from a glass enclosed 6AH6 receiving tube. This tube has a rectangular cathode, 3- by 10-mm, and planar grids. The separation between cathode and control grid is about 1 mm, as is that between the two grids. Thus, the excitation region is quite small. Coils external to the vacuum system furnish a magnetic field of 10-100 gauss at the electron gun; this field provides additional confinement of the excitation region.

The electron gun is pulsed by applying a negative voltage pulse to the cathode, with both grids at electrical ground. Commercial pulse generators are used to provide negative rectangular voltage pulses variable in both height and width. Pulse heights from 20 to 200 volts and widths from 0.4 to 8.0 μsec are used in the present experiment.

C. Detectors

The detector depicted in Fig. 1 (labelled CEM) is a continuous dynode, windowless electron multiplier (Channeltron, Bendix Model 450). The CEM is sensitive to photons, ions, metastables, energetic ground state neutrals, and electrons. The entrance horn of the CEM is negatively biased to discriminate against negative ions while the position of the CEM is arranged to avoid detection of photons, emitted either at the electron gun or along the flight path. Thus, as indicated in Fig. 1, the CEM is "hidden from view" from the electron gun and most of the flight path; therefore, it is sensitive primarily to events occurring near the end of the flight path.

It is also desirable to prevent the detection of any positive ions produced in the electron gun. This is achieved by applying appropriate dc voltages to a pair of small parallel plates located midway between the electron gun and the detector. These plates are labelled CHARGE REMOVAL REGION in Fig. 1.

The tilted straight line at the end of the flight path in Fig. 1 represents a flat 1-cm square stainless steel plate which is placed in front of the CEM horn, at an angle of about 45° with respect to the center line of the flight path. This plate serves to effectively terminate the flight path for photons, which are mostly absorbed by the plate, and for metastable neutral atoms and molecules, which are quenched at the plate. Both photons and metastables can eject electrons from the plate, and sometimes the metastables can also be ionized at or near the surface.[12,13] If the CEM horn is positively biased, then photoelectrons and Auger electrons will be detected. However, with the CEM biased sufficiently negative, positive ions created either by surface ionization[12,13] or by electric field ionization[12,14,15] are detected.

In the present experiment, time-of-flight spectra obtained with the CEM negatively biased are strictly attributable to positive ion formation at the detector plate, whereas with a positive bias on the CEM the spectra appear to be contaminated by electrons created in other parts of the apparatus, e.g., at or near the ion removal region. Thus, all TOF spectra were obtained with the CEM biased at -1 kV.

Later, it became desirable to improve the resolution of the apparatus, i.e., to reduce a time-of-flight "linewidth" due to the finite size of the excitation and detection regions. Therefore,

the CEM was replaced with a small magnetic electron multiplier (Bendix Model M308, labelled MEM in Fig. 2), and the stainless steel plate was replaced by a short length of #12 copper wire (see Fig. 2). The entrance grid of the MEM is negatively biased at -1.6 kV so that the MEM also detects only positive ions, instead of Auger electrons.

IV. TIME-OF-FLIGHT SPECTRA

A time-of-flight spectrum obtained using either configuration of the apparatus should represent primarily the flight of metastable atoms or molecules through a distance of about 15 cm. (In Fig. 1, the mean flight path is 14.7 cm and, in Fig. 2, it is 15.3 cm.) A typical TOF spectrum for nitrogen atoms, obtained with the apparatus of Fig. 1, is shown in Fig. 3. There, the most probable time of flight is 22 μsec, corresponding to a speed of 0.7×10^6 cm/sec. The magnitude of the most probable velocity is somewhat smaller than this since the velocity distribution P(v) is related to the time-of-flight spectrum P(t) by

$$P(v) \propto v^{-2} P(t).$$

Nonetheless, all the velocities represented in Fig. 3 are large compared with the ambient mean thermal velocity of N_2 molecules. Therefore, it is concluded that the spectrum of Fig. 3 is due entirely to metastable N atoms produced by electron impact dissociative excitation of N_2. This spectrum has an appearance threshold, in electron bombardment energy, of approximately 26 eV, and it is essentially unaltered in shape throughout the energy range 30 -50 eV. Data showing the detailed dependence of a oxygen TOF spectrum upon electron bombardment energy have been published[4,5].

Using the higher resolution apparatus (Fig. 2) and bombardment energies of the order of 100 eV, more complex TOF spectra are obtained, as is indicated by the spectra shown in Fig. 4. There, the peak occurring at a TOF of 21 μsec probably corresponds to the single peak in Fig. 3; but the peak at 16 μsec is either not present or is unresolved in the lower energy spectrum. It is this fast peak

which contains a large number of nitrogen atoms in non-Rydberg levels, as is shown in the following two sections.

V. LIFETIME MEASUREMENT

A priori, the TOF spectra shown in Figs. 3 and 4 most likely represent nitrogen atoms in Rydberg levels,[4,5,10] since the low lying ^2D and ^2P metastable states of N are probably not detected in the present apparatus, and since the $2s(2p)^3 3s\ ^6S_{5/2}$ metastable auto-ionizing state of N has never been observed, although its existence has been discussed.[16-20] However, in the strictest sense, the TOF spectra just described can represent atoms in any or all of the metastable states of N; therefore, a lifetime measurement was used to provide additional specification. The natural lifetimes for the ^2D and ^2P levels of N are known[21]; they are 26 hr and 12 sec, respectively. Atoms in Rydberg levels should exhibit a variety of lifetimes,[14,22] dependent upon excitation conditions and the effects of collisional quenching[23]; they range from 1 to 100 μsec.

The apparatus used for the lifetime measurement is located at the University of California, Berkeley, and has been described in detail previously.[24] This apparatus, although similar to the one described above, differs in that TOF spectra are accumulated by two detectors (instead of one) located at two different positions along the flight path. At the first detector, 68 cm from the electron gun, the flight path is intersected by a 60% transparent metallic mesh, and Auger electrons produced at the mesh are collected by an electron multiplier in essentially the manner indicated in Fig. 1. The flight path is then terminated by a solid metal plate and second electron multiplier, located 183 cm from the electron gun.

For atoms or molecules in relatively short lived metastable

states, the TOF spectra accumulated at the two detectors in the lifetime apparatus differ due to in-flight decay along the flight path between the two detectors.[24] If only one metastable species is present in the atomic beam, its lifetime can be obtained from a comparison of the two spectra. Specifically, the number of atoms, $N_2(t_2)$, detected at the second detector at time t_2, is related to the arrival of $N_1(t_1)$ atoms at the first detector, at the corresponding earlier time, t_1, by the equation

$$N_2(t_2) = C\, N_1(t_1)\, \exp[-(t_2 - t_1)/\tau] \ ,$$

where C is a constant whose value depends upon the relative efficiencies of the two detectors[24], and τ is the natural lifetime of the metastable state. For clarity it is noted that $t_2 - t_1 = (L_2 - L_1)/v$, where $L_2 - L_1$ is the separation of the two detectors and v is the magnitude of an initial velocity, given by $t_1 = L_1/v$, or by $t_2 = L_2/v$. The lifetime, τ, is obtained by evaluating, for the same velocity interval, the point-by-point ratio of the two spectra, and plotting

$$\ell n(N_2/N_1) = \ell n\, C - (t_2 - t_1)/\tau \ , \qquad (1)$$

as a function of $(t_2 - t_1)$. The slope of the resulting straight line is $-1/\tau$.

The data storage unit in the lifetime apparatus has a minimum channel width of 8.25 μsec; therefore, although the flight path is longer, the TOF resolving power of this apparatus is less than that of the apparatus shown in Figs. 1 and 2. Consequently, the TOF spectra for the metastable atoms produced by dissociative excitation of N_2 are not cleanly resolved from contaminant spectra.[25] However,

comparison with the spectra taken at higher resolution (as in Fig. 4, for example) allows unambiguous identification.

A plot of Eq. (1), for nitrogen data, is shown in Fig. 5. Although the data are too scattered to allow specification of a single exponential decay, it is clear that the decay is dominated by components with lifetimes of the order of 100 μsec; therefore, the observed TOF spectra do not represent, to any significant extent, nitrogen atoms in the ^2D and ^2P metastable states. Further, because of the effects of collisional quenching in the excitation region, it is also highly unlikely that these spectra are due to nitrogen atoms in Rydberg levels. As has been discussed,[24] the background gas pressure along the flight path between detectors is always less than 10^{-8} Torr; however, in the excitation region, the operating pressure is typically 5×10^{-6} Torr or higher. Since the distance between the excitation region and the entrance aperture to the flight path is 10 cm, collisional quenching of Rydberg atoms can be extremely important in this region. For example, an s-state Rydberg atom with a lifetime of 100 μsec has a principal quantum number $n \simeq 35$; therefore, its gas kinetic mean free path in N_2 at 5×10^{-6} Torr is $\lambda \simeq 3\times10^{-2}$ cm. Thus, if collisional quenching cross sections are comparable with or larger than[23] geometrical cross sections, all Rydberg atoms with natural lifetimes greater than 1 μsec have a very low probability for escaping from the excitation region of the lifetime apparatus. On the other hand, metastable atoms with natural lifetimes shorter than 1 μsec must live for approximately 100 lifetimes to reach the nearest detector in this apparatus, and these atoms certainly cannot contribute significantly to the decay curve shown in Fig. 5.

VI. QUENCHING BY A STATIC ELECTRIC FIELD

A static electric field of magnitude E between the quench plates shown in Fig. 2 will decrease the lifetime of a metastable atom travelling along the flight path. The effect of this quenching field upon the time-of-flight spectrum for a single metastable state i can be described as[26]

$$N_i(t,E) = N_{0i} \exp\{-[\gamma_{0i} + (D/L)\gamma_i(E)]t\} , \qquad (2)$$

where t is time-of-flight, γ_{0i} is the natural decay constant for the i^{th} state, $\gamma_i(E)$ is the field dependent decay constant (i.e., $\gamma_i(0) = 0$), D is the length of the quench plates, L is the total length of the flight path, and N_{0i} is the number of atoms created in the i^{th} state with a velocity of magnitude $v = L/t$. The TOF spectra obtained for two different values of quench field, E_1 and E_2, are related by the expression

$$N_i(t,E_2)/N_i(t,E_1) = \exp\{-(D/L)[\gamma_i(E_2) - \gamma_i(E_1)]t\} .$$

With $E_1 = 0$, a plot of $\ell n\, R(t,E) = \ell n[N_i(t,E)/N_i(t,0)]$, as a function of flight time, determines $\gamma_i(E)$; therefore, the functional dependence of $\gamma_i(E)$ can be determined by comparing TOF spectra for different values of the quench field. A determination of the dependence of $\gamma_i(E)$ upon E aids in the identification of metastable states, because, as is now discussed, a qualitative difference is expected between Rydberg and non-Rydberg levels.

A. Quenching Theory for Rydberg Levels

Classically, an applied electric field is expected to have a step function effect upon the lifetime of an atom in a Rydberg level;

if the electric field is strong enough to field ionize the atom, the lifetime is lowered drastically, otherwise it is essentially unaffected by the field. In this picture, the average time required for field ionization is of the same order of magnitude as the period of the unperturbed motion, which is orders of magnitude smaller than a typical time-of-flight for any Rydberg atom observable with the present apparatus. For example, in the Rydberg levels with $n \simeq 100$ the period of a circular orbit is approximately 10^{-12} sec. compared to a time-of-flight of about 10^{-5} sec.

Similar results are obtained for hydrogen when the problem is treated quantum mechanically.[27] For example, the field ionization probability of the most readily ionized states in the n = 25 levels of H increases from 10^{5} sec^{-1} to 10^{11} sec^{-1} as the strength of the electric field increases from 1.5 kV/cm to 1.8 kV/cm. Therefore, for highly excited hydrogen levels, the field dependent decay constant, $\gamma_i(E)$, in Eq. 2 can be expressed as

$$\gamma_i(E) \simeq \begin{cases} 0, & \text{if } E < E_{ci} \\ \infty, & \text{if } E > E_{ci} \end{cases},$$

where E_{ci} is a critical electric field strength, above which field ionization occurs. Thus, the TOF spectrum for hydrogen atoms in a single Rydberg state should either be unaffected by the electric field or completely quenched, <u>independent</u> of time-of-flight.

The theory of field ionization of a hydrogen Rydberg is also applicable to the lowest $(2s)^2(2p)^2 n\ell$ Rydberg levels in nitrogen if configuration mixing is neglected. However, the most important contribution to configuration mixing can be taken into account in a fairly precise way, and as shown in the appendix, field ionization in nitrogen is essentially unaffected by configuration

mixing. Therefore, the field ionization of the Rydberg levels of nitrogen should be qualitatively the same as for the corresponding levels of hydrogen.

B. Quenching Theory for the $2s(2p)^3\ 3s\ ^6S_{5/2}$ State of Nitrogen

The effect of an applied electric field upon the lifetime of the $2s(2p)^3\ 3s\ ^6S_{5/2}$ metastable auto-ionizing state of N is expected to differ qualitatively from the results just described for Rydberg levels. This expectation is independent of the exact energy location of the ^6S state, but it can be assumed to be 17.2 eV above the ground state,[17] in the first ionization continuum. Then to first order, an electric field does not cause mixing of the $3s\ ^6S$ state with the degenerate continuum states because of the selection rule forbidding two-electron jumps.[29] However, the electric field will cause a mixing of the $2s(2p)^3\ 3s$ and $2s(2p)^4$ configurations. Therefore, the field dependent decay constant for the $3s\ ^6S$ state is given approximately by[26,32]

$$\gamma_6(E) = \gamma_{06} + (D/L)k_6E^2 ,$$

where k_6 is a constant representing the details of the configuration mixing and γ_{06} is the natural decay constant.

C. Quenching Results

Electric field quenching of the nitrogen metastables is achieved by applying appropriate voltages to a pair of 3- by 6-cm parallel plates (see Fig. 2). The long dimension of the plates is parallel to the flight path. The separation, d, of the plates is approximately 1 cm. Typical voltages applied to the lower and upper field plates

are listed in the columns labelled V_L and V_U in Fig. 4. It is necessary to use a non-symmetric combination of V_L and V_U in order to minimize contamination[25] of the TOF spectra. The TOF data shown in Fig. 4 represent quenching field strengths of 0.0, 0.5, 2.0, and 4.0 kV/cm. The lowest applied voltages do not provide a field free flight path because a fringing field still exists. This fringing field is unimportant for Rydberg atoms because a Rydberg atom is unaffected by the electric field until a critical field is reached, and then it is field ionized. However, for non-Rydberg atoms, the fringing field requires that the argument of the exponential function in Eq. (2) be replaced by the expression

$$-[\gamma'_{oi}(E_f) + (D'/L)\gamma_i(E)]t \quad ,$$

where γ'_{oi} is independent of applied electric field, E_f is the fringing field, and $D' > D$.

The three logarithmic plots of $N(t,E)/N(t,E_f)$ for the data of Fig. 4 are shown in Fig. 6. The three straight lines in Fig. 6 represent an estimate of initial slope of the plots and correspond to the fastest atoms. The important point is that the electric field quenching is not entirely independent of time-of-flight. Therefore, it is concluded that the observed TOF spectrum contains, in addition to a sizeable contribution from Rydberg atoms, at least one non-Rydberg component.

At the electron bombardment energy used to obtain the spectra shown in Fig. 4, it is probable that each metastable atomic state can originate from more than one dissociative molecular state. Consequently, there may be more than one initial velocity distribution and TOF spectrum for each atomic state. If the dissociative cross

sections are different, there will be a distinct value of N_{oi} for each dissociative state, and the right hand side of Eq. (2) becomes a sum of terms.

Unfortunately, the precision of the data shown in Fig. 6, representing about 40 hrs of collection time, is insufficient to warrant quantitative analysis. Therefore, it is regarded as fortunate that the fast atoms in the TOF spectrum appear to be dominated by a single velocity distribution representing a single metastable non-Rydberg state. (This result is consistent with the lifetime measurement discussed in Section V.) The slower peak appearing at 29 μsec in Fig. 6 is probably due to a second distinct velocity distribution for a non-Rydberg state. Figure 7 is a plot of the initial measured slopes, $(D'/L)\gamma(E)$, of the straight lines shown in Fig. 6 as a function of E^2. Also shown is the same kind of plot for additional sets of data. These plots show that quenching of the fastest atoms varies as E^2 and indicate qualitative agreement with the theory described above for the quenching of the $2s(2p)^3\ 3s\ ^6S_{5/2}$ metastable state of nitrogen. The differences in slopes and intercepts in Fig. 7 arise from different fringing fields for the various data sets.

VII. CONCLUSIONS

If the lifetime measurement described here corresponds to the natural decay of nitrogen atoms in Rydberg levels, then the collisional quenching cross sections for these atoms, in the parent N_2 gas, must be very much smaller than the geometrical cross sections. In contrast, previous work indicates the reverse to be true. The conclusion is that the measurement is the lifetime of the $2s(2p)^3 3s\ ^6S_{5/2}$ mestastable auto-ionizing state.

The electric field quenched TOF spectra correspond to at least two different types of metastable atomic states. For one of these the fractional quenching in a given electric field is independent of TOF. For the other, the quenched TOF spectrum decays approximately exponentially with increasing TOF, and the measured decay constant is proportional to the square of the electric field. Therefore, if the observed TOF spectra correspond only to nitrogen atoms in Rydberg levels, there are two distinct types of nitrogen Rydberg levels. For one of these, the electric field quenching is the same as for hydrogen; i.e., configuration mixing is unimportant. For the other type, the electric field quenching is due primarily to the effects of configuration mixing in violation of the general selection rules for configuration mixing.[29] In contrast, if the general selection rules for configuration mixing are <u>not</u> violated, then the field dependent decay constant for the $2s(2p)^3\ 3s\ ^6S_{5/2}$ state of N is predicted to vary quadratically with electric field strength, as pointed out in the previous section.

There is no reason to believe that Rydberg levels in atomic nitrogen are anomalous in either their collisional quenching or their electric field quenching. Therefore, it is concluded, instead, that

in the range of bombardment energies where the production of Rydberg atoms by electron impact dissociation of N_2 is important, the production of nitrogen atoms in the $2s(2p)^3\ 3s\ ^6S_{5/2}$ metastable auto-ionizing state is also important. Furthermore , the natural lifetime of this state is 100 ± 25 μsec.

ACKNOWLEDGEMENTS

The authors are grateful to Dr. Howard Shugart for his encouragement of the lifetime measurement, and to Dr. Mel Simmons for his assistance in acquisition of the lifetime data. One of us (CEJ) enjoyed the hospitality of the Oregon State University Department of Physics during part of this work.

Appendix

For the $(2s)^2\ (2p)^2\ n\ell$ Rydberg levels in nitrogen, the predominant contribution to configuration mixing should come from the four levels in the $2s(2p)^4$ configuration.[28,30] The lowest two levels (^4P, ^2P) lie approximately 10 eV above the ground state,[30] and the upper two (^2D, ^2S) are predicted to lie in the first ionization continuum.[31] Because of the selection rules for configuration mixing,[28] all of the odd parity $(2s)^2\ (2p)^2\ n\ell$ levels, and many of those with even parity do not mix, in first order, with the $2s(2p)^4$ configuration. The natural lifetimes for the remainder of these levels should be shortened by the effects of mixing, since the states in the $2s(2p)^4$ configuration decay by resonance transitions to the $(2s)^2\ (2p)^3$ configuration.

The situation just described is essentially unaltered by the addition to the problem of an applied electrostatic field, because, to lowest order, this perturbation does not mix states having different single particle quantum numbers for more than one electron.[29] Therefore, the $(2s)^2\ (2p)^2\ n\ell$ - $2s(2p)^4$ configuration mixing is altered very little by application of an electrostatic field. Consequently, the theory of field ionization of H should also apply fairly well to the $(2s)^2\ (2p)^2\ n\ell$ Rydberg levels of N.

REFERENCES

*Work supported by the Atmospheric Sciences Section, National Science Foundation .

†Work supported by the U. S. Atomic Energy Commission. Present address: Department of Physics, North Carolina State University, Raleigh, North Carolina 27607 .

1. M. Leventhal, R. T. Robiscoe, and K. R. Lea, Phys. Rev. 158, 49 (1967).

2. R. Clampitt and A. S. Newton, J. Chem, Phys. 50, 1997 (1969).

3. J. W. Czarnik and C. E. Fairchild, Phys. Rev. Lett. 26, 807 (1971).

4. R. S. Freund, J. Chem. Phys. 54, 3125 (1971).

5. W. L. Borst and E. C. Zipf, Phys. Rev. A4, 153 (1971).

6. W. C. Wells, W. L. Borst, and E. C. Zipf, J. Geophys. Res. 77, 69 (1972).

7. M. Misakian and J. C. Zorn, Phys. Rev. A6, 2180 (1972).

8. C. E. Johnson, J. Chem. Phys. 57, 576 (1972).

9. For a review of various aspects of the dissociation and dissociative excitation of simple molecules, see Proceedings of the Workshop on Dissociative Excitation of Simple Molecules, L. J. Kieffer (editor), JILA Information Center Report No. 12 (unpublished) (1972).

10. W. C. Wells, W. L. Borst, and E. C. Zipf, in Seventh International Conference on the Physics of Electron and Atomic Collisions, Amsterdam, The Netherlands, 1971 (North-Holland, Amsterdam, 1971), p. 576.

11. C. E. Fairchild, Bull. Am. Phys. Soc. 17, 132 (1972).

12. S. E. Kuprianov, Zh. Eksp. Teor. Fiz. Pisma 5, 245 (1967). [Sov. Phys. JEPT Lett. 5, 197 (1967)].

13. A. V. Chaplik, Zh. Eksp. Teor. Fiz. 54, 332 (1968). [Sov. Phys. JETP 27, 178 (1968)].

14. N. V. Federenko, V. A. Andukinov, and R. N. Il'in, Zh. Tekn. Fiz. 35, 585 (1965) [Sov. Phys. Tech. Phys. 10, 461 (1965)].

15. E. S. Solov'ev, R. N. Il'in, V. A. Oparin, I. T. Serenkov, and N. V. Federenko, Zh. Eksp. Teor. Fiz. Pisma 10, 300 (1969) [Sov. Phys. JETP Lett. 10, 190 (1969)].

16. F. R. Innes and O. Oldenberg, J. Chem. Phys. 37 2427 (1962).

17. A. B. Prag and K. C. Clark, J. Chem. Phys. 39, 799 (1963).

18. R. A. Young, R. L. Sharpless, and R. Stringham, J. Chem. Phys. 40, 117 (1964).

19. K. M. Evenson and D. S. Burch, J. Chem. Phys. 45, 2450 (1966).

20. O. Oldenberg, Physical Sciences Research Papers, No. 323 (Office of Aerospace Research, United States Air Force) (1967, unpublished).

21. A. N. Wright and C. A. Winkler, Active Nitrogen (Academic Press, New York, 1968), Chapter 3.

22. H. A. Bethe and E. E. Salpeter, Quantum Mechanics of One and Two Electron Atoms (Springer, Berlin, 1957).

23. M. Matsuzawa, J. Chem. Phys. 55, 2685 (1971).

24. R. S. Van Dyck, C. E. Johnson, and H. A. Shugart, Phys. Rev. A4, 1327 (1971).

25. For both apparatuses used in the present experiment there are one or more (depending upon electron gun voltages) unidentified very fast peaks in the TOF spectra. These peaks are probably due to neutral atoms and molecules produced by charge exchange of fast ions in the excitation region. See also C. E. Johnson, Phys. Rev. A5, 2688 (1972).

26. C. E. Johnson, Phys. Rev. A (March, 1973).

27. D. S. Bailey, J. R. Hiskes, and A. C. Riviere, Nuc. Fusion 5, 41 (1965).

28. E. U. Condon and G. H. Shortley, The Theory of Atomic Spectra (University Press, Cambridge, 1935), Chapter XV.

29. Ibid., p. 375.

30. H. G. Kuhn, Atomic Spectra (Academic Press, second edition, New York, 1969).

31. C. A. Nicolaides. Phys. Rev. A6, 2078 (1972).

32. L. I. Schiff, Quantum Mechanics (McGraw-Hill, Inc., New York, second edition, 1955), Chapters VII, X.

Figure Captions

Fig. 1. Outline of the low resolution time-of-flight apparatus.

Fig. 2. Outline of the high resolution time-of-flight apparatus.

Fig. 3. A low resolution time-of-flight spectrum. The solid line represents a qualitative interpretation of the data, which were accumulated during a two hour period.

Fig. 4. High resolution time-of-flight spectra. The four spectra were obtained using four different voltages applied to the electric field quenching plates shown in Fig. 2, giving four different quenching fields. For example, the open circles in the figure represent an applied electric quenching field of 4 kV/cm.

Fig. 5. Decay plot. The point-by-point ratio of the time-of-flight spectra accumulated at the two separate detectors used for a measurement of the lifetime τ. The straight line, whose slope = $-1/\tau$, is a qualitative interpretation of the data.

Fig. 6. Quench plots. The point-by-point ratios of the time-of-flight spectra shown in Fig. 4. The ratios plotted are those for each of the lower three spectra of Fig. 4 to the uppermost spectrum. For the uppermost spectrum, the quench plates are biased equally; therefore, only an unknown fringing field, E_f, remains. The straight lines in the figure represent an estimate of the initial slopes (see Eq. 2).

Fig. 7. Dependence of the measured decay constants on the square of the electric quenching field. The solid circles are obtained using Eq. 2 and the time-of-flight spectra of Fig. 6, while the open circles, open triangles, and crosses represent three additional sets of data, which have different residual fringing fields.

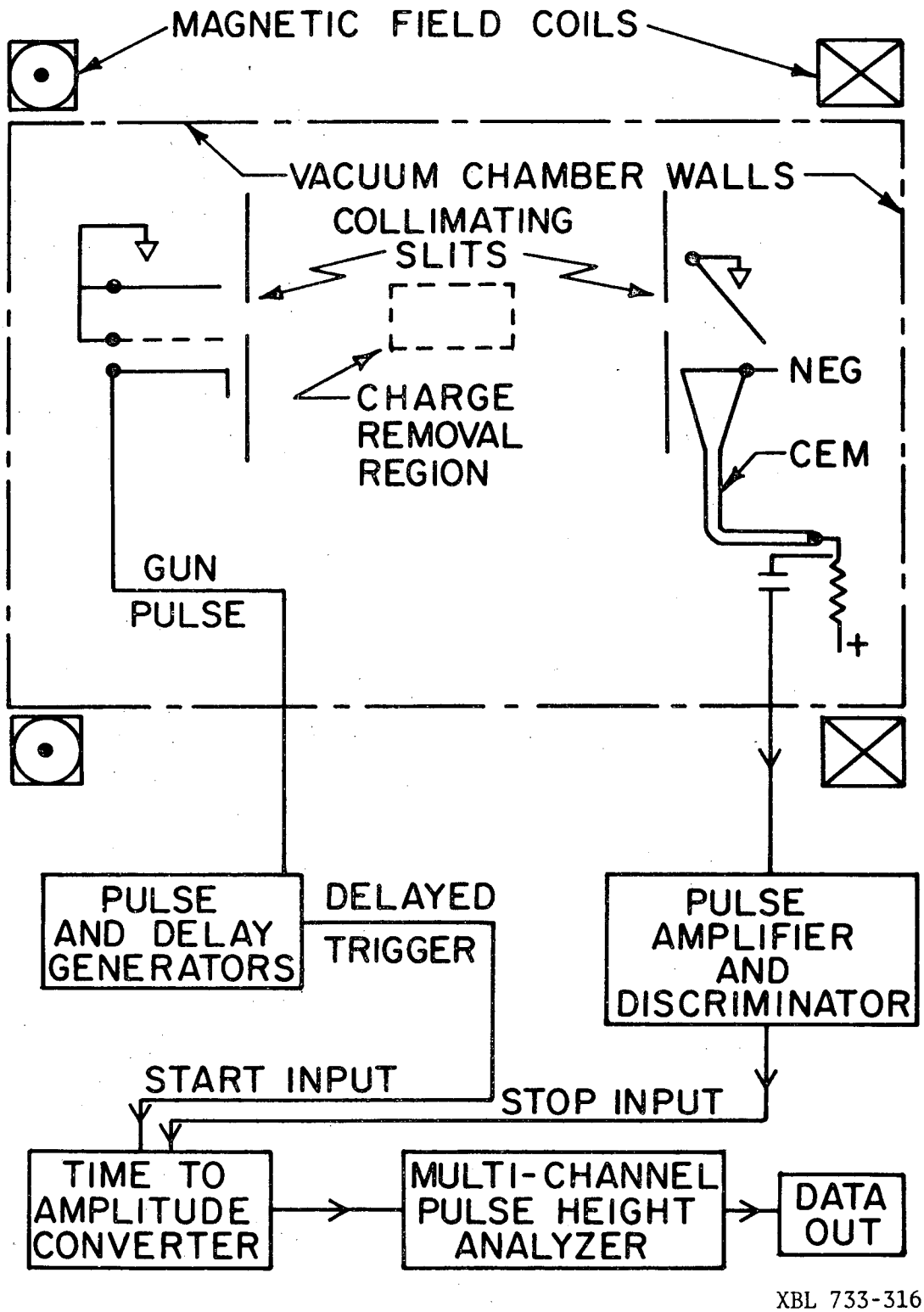
MAGNETIC FIELD COILS
VACUUM CHAMBER WALLS
COLLIMATING SLITS
CHARGE REMOVAL REGION
NEG
CEM
GUN PULSE
+
PULSE AND DELAY GENERATORS
DELAYED TRIGGER
PULSE AMPLIFIER AND DISCRIMINATOR
START INPUT
STOP INPUT
TIME TO AMPLITUDE CONVERTER
MULTI-CHANNEL PULSE HEIGHT ANALYZER
DATA OUT
XBL 733-316

Fig. 1

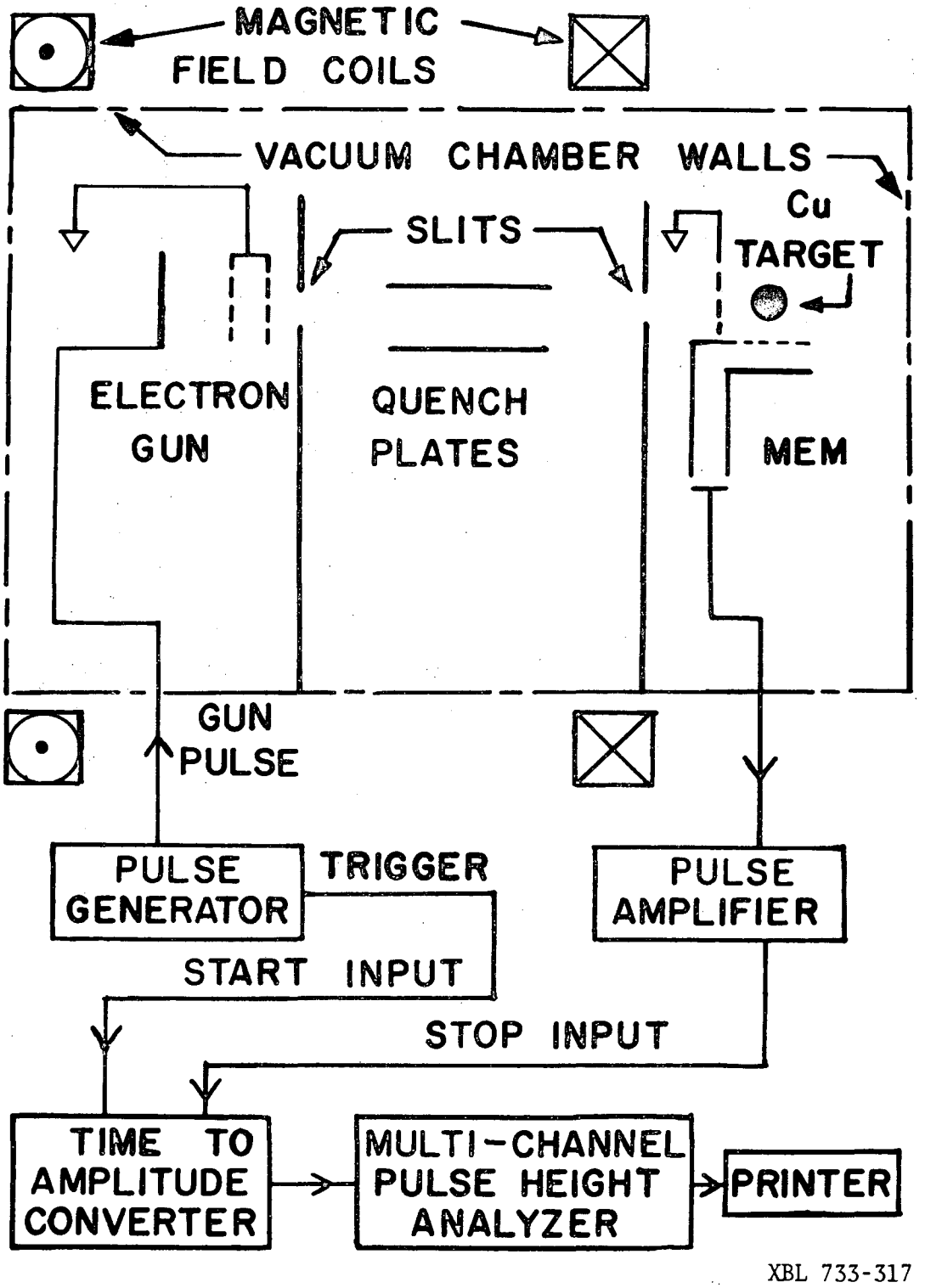
MAGNETIC
FIELD COILS
VACUUM CHAMBER WALLS
SLITS
Cu
TARGET
ELECTRON
GUN
QUENCH
PLATES
MEM
GUN
PULSE
PULSE
GENERATOR
TRIGGER
PULSE
AMPLIFIER
START INPUT
STOP INPUT
TIME TO
AMPLITUDE
CONVERTER
MULTI-CHANNEL
PULSE HEIGHT
ANALYZER
PRINTER
XBL 733-317

Fig. 2

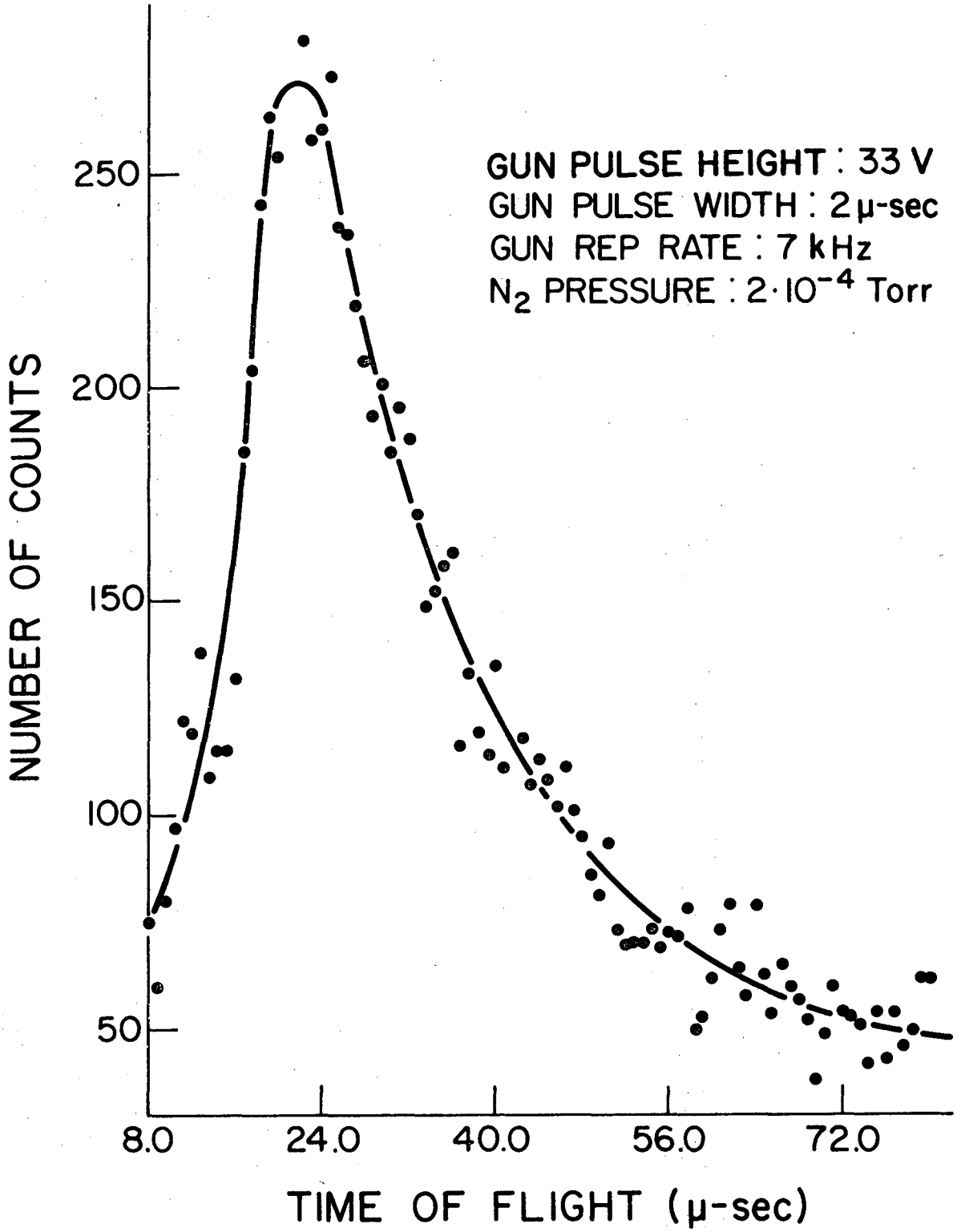

XBL 733-318

Fig. 3

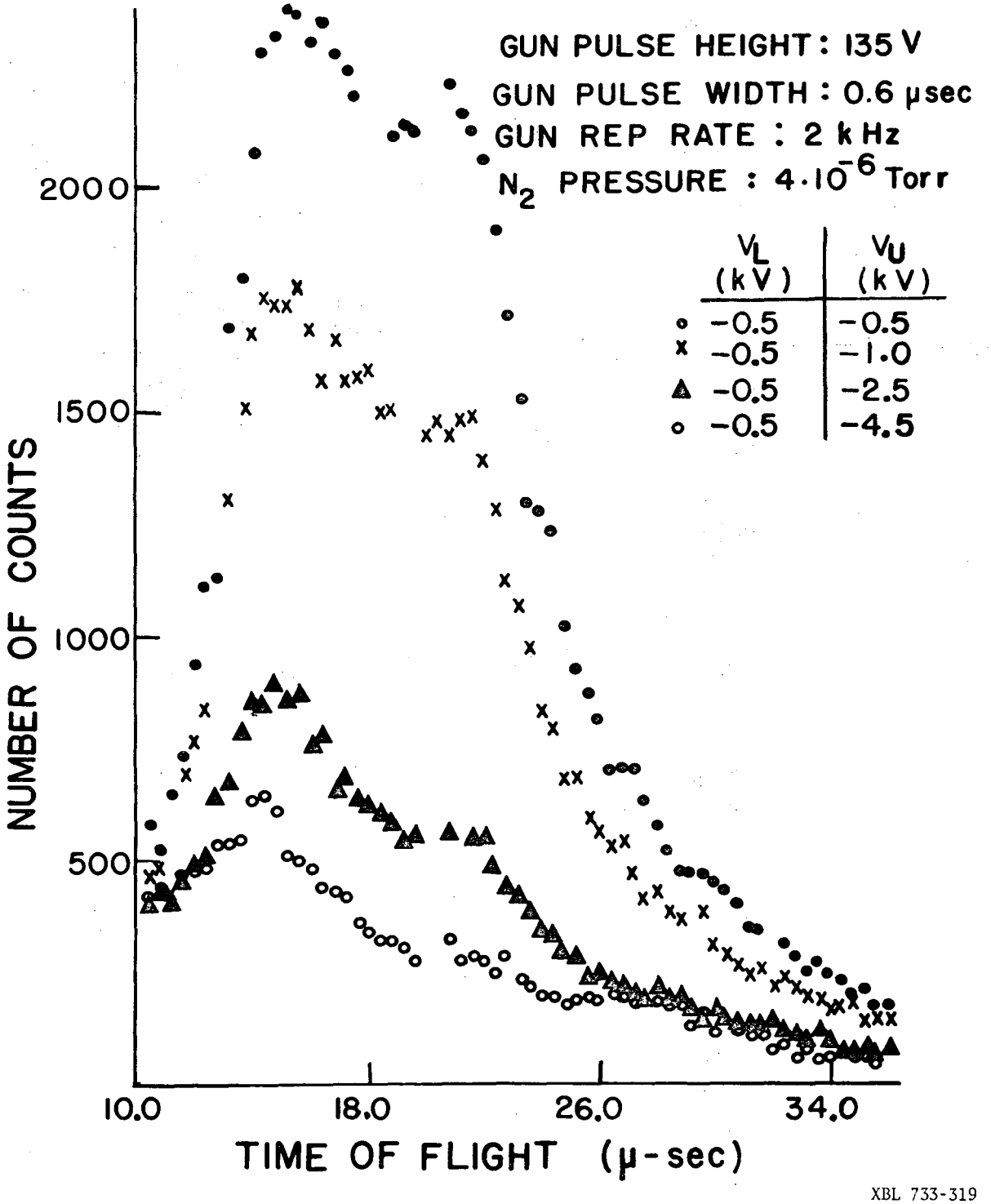
GUN PULSE HEIGHT: 135 V
GUN PULSE WIDTH: 0.6 μsec
GUN REP RATE: 2 kHz
N2 PRESSURE: 4·10-6 Torr
VL (kV)
VU (kV)
-0.5
-0.5
-0.5
-0.5
-0.5
-1.0
-2.5
-4.5
NUMBER OF COUNTS
2000
1500
1000
500
10.0
18.0
26.0
34.0
TIME OF FLIGHT (μ-sec)
XBL 733-319

Fig. 4

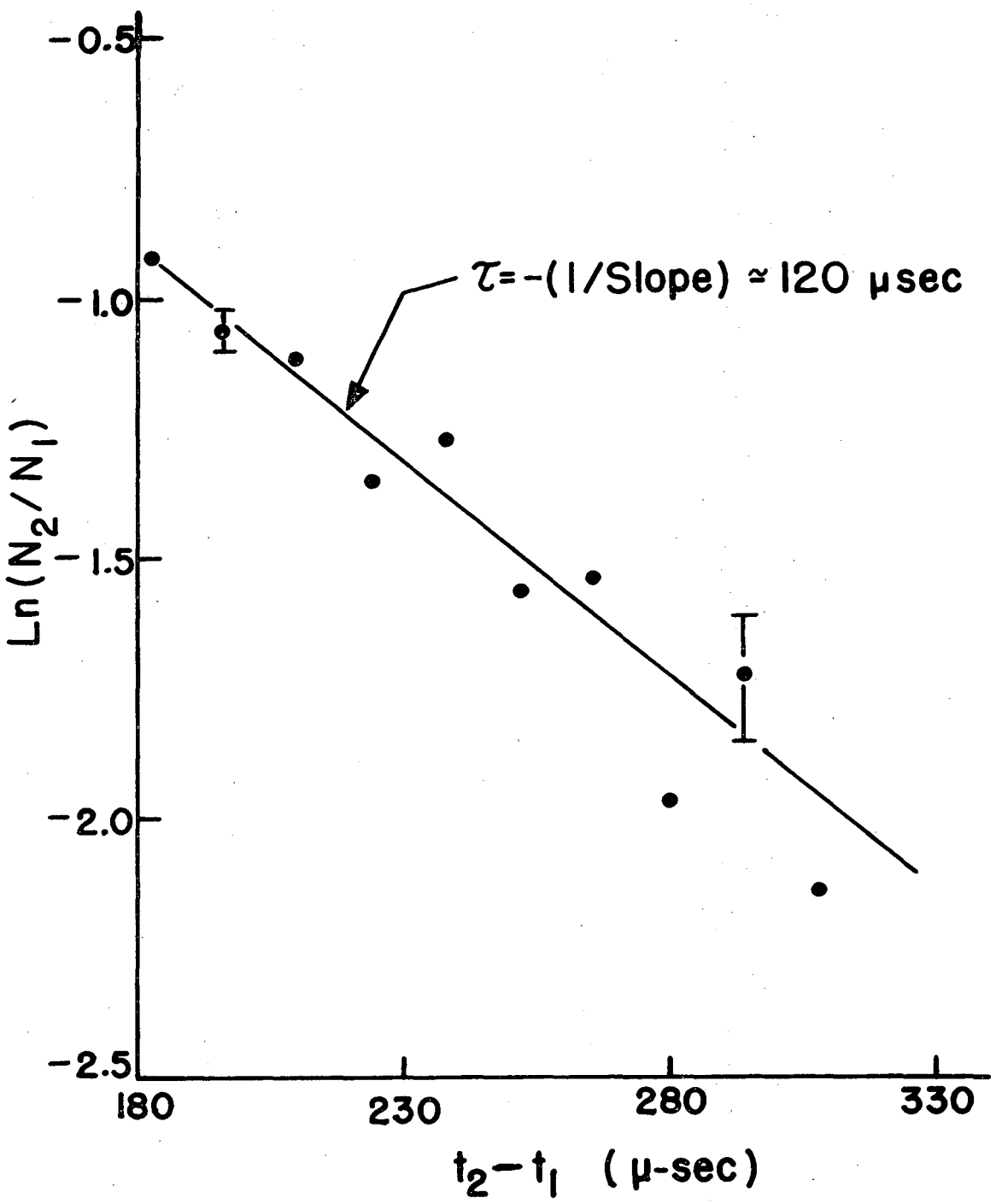
-0.5
-1.0
-1.5
-2.0
-2.5
Ln (N2/N1)
τ=-(1/Slope) ≈ 120 μsec
180
230
280
330
t2-t1 (μ-sec)
XBL 733-322

Fig. 5

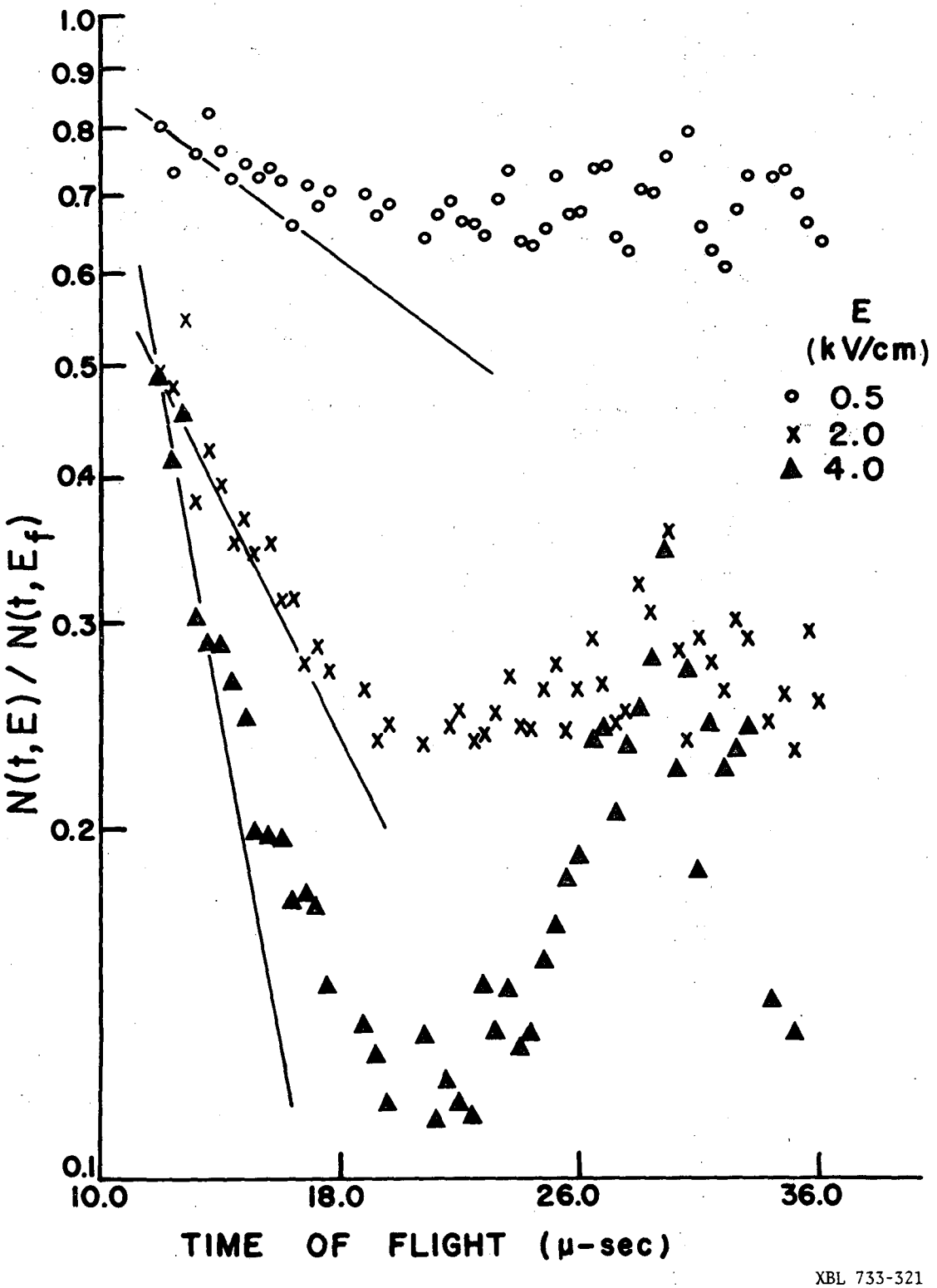
1.0
0.9
0.8
0.7
0.6
0.5
0.4
0.3
0.2
0.1
N(t,E) / N(t,Ef)
E
(kV/cm)
0.5
2.0
4.0
10.0
18.0
26.0
36.0
TIME OF FLIGHT (μ-sec)
XBL 733-321

Fig. 6

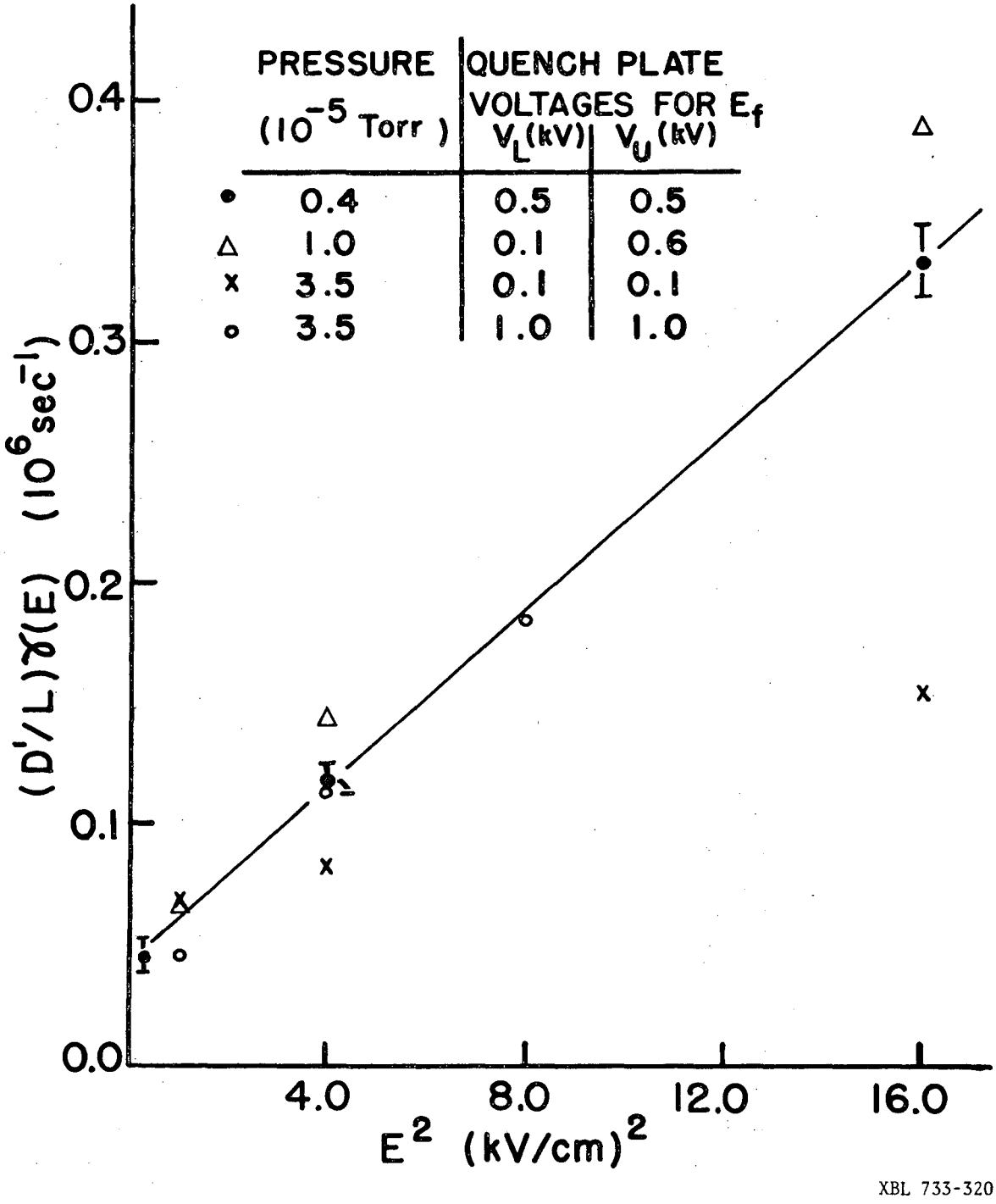
PRESSURE (10^{-5} Torr)
QUENCH PLATE VOLTAGES FOR E_f
V_L(kV)
V_U(kV)
0.4 0.5 0.5
1.0 0.1 0.6
3.5 0.1 0.1
3.5 1.0 1.0
$(D'/L)\gamma(E)$ (10^6 sec^{-1})
0.0
0.1
0.2
0.3
0.4
4.0
8.0
12.0
16.0
E^2 (kV/cm)^2
XBL 733-320

Fig. 7

TECHNICAL INFORMATION DIVISION
LAWRENCE BERKELEY LABORATORY
UNIVERSITY OF CALIFORNIA
BERKELEY, CALIFORNIA 94720